1 Improving the Generation and Selection of Virtual Populations

2 in Quantitative Systems Pharmacology Models

- 3 Theodore R. Rieger¹, Richard J. Allen¹, Lukas Bystricky², Yuzhou Chen³, Glen Wright
- 4 Colopy⁴, Yifan Cui⁵, Angelica Gonzalez⁶, Yifei Liu⁷, R. D. White⁸, R. A. Everett⁸, H. T.
- 5 Banks⁸, Cynthia J. Musante¹
- 6
- ⁷ ¹Internal Medicine Research Unit, Pfizer Inc, Cambridge, MA, USA
- 8 ²Department of Computer Science, Florida State University, Tallahassee, FL, USA
- 9 ³Department of Mathematical Sciences, University of Texas-Dallas, Dallas, TX, USA
- 10 ⁴Institute of Biomedical Engineering, Department of Engineering Science, University
- 11 of Oxford, Oxford, UK
- 12 ⁵Department of Statistics and Operations Research, University of North Carolina-
- 13 Chapel Hill, Chapel Hill, NC, USA
- 14 ⁶Department of Mathematics, University of Arizona, Tucson, AZ, USA
- 15 ⁷Department of Statistics, University of Wisconsin-Madison, Madison, WI, USA
- 16 ⁸Center for Research in Scientific Computation, North Carolina State University,
- 17 Raleigh, NC, USA
- 18

19 *** Correspondence**:

- 20 Theodore Rieger
- 21 ted.rieger@pfizer.com

22 Abstract

23 Quantitative systems pharmacology (QSP) models aim to describe mechanistically

- 24 the pathophysiology of disease and predict the effects of therapies on that disease.
- 25 For most drug development applications, it is important to predict not only the
- 26 mean response to an intervention but also the distribution of responses, due to
- 27 inter-patient variability. Given the necessary complexity of QSP models, and the
- sparsity of relevant human data, the parameters of QSP models are often not well
- determined. One approach to overcome these limitations is to develop alternative
- 30 virtual patients (VPs) and virtual populations (Vpops), which allow for the
- 31 exploration of parametric uncertainty and reproduce inter-patient variability in
- 32 response to perturbation. Here we evaluated approaches to improve the efficiency
- 33 of generating Vpops. We aimed to generate Vpops without sacrificing diversity of
- 34 the VPs' pathophysiologies and phenotypes. To do this, we built upon a previously
- 35 published approach (Allen, Rieger et al. 2016) by (a) incorporating alternative
- 36 optimization algorithms (genetic algorithm and Metropolis-Hastings) or
- 37 alternatively (b) augmenting the optimized objective function. Each method
- 38 improved the baseline algorithm by requiring significantly fewer plausible patients
- 39 (precursors to VPs) to create a reasonable Vpop. #ddct #qsp
- 40

41 **1 Keywords**

- 42 Global optimization, acceptance rejection sampling, mathematical modeling,
- 43 ordinary differential equations, genetic algorithm, Metropolis-Hastings

44 2 Abbreviations

- 45 GA Genetic Algorithm
- 46 GoF Goodness of Fit
- 47 HDL_c High Density Lipoprotein Cholesterol
- 48 LDL_c Low Density Lipoprotein Cholesterol
- 49 MH Metropolis-Hastings
- 50 NHANES National Health And Nutrition Examination Survey
- 51 NSA Nested Simulated Annealing
- 52 SA Simulated Annealing
- 53 PP Plausible Patient
- 54 QSP Quantitative Systems Pharmacology
- 55 TC Total Cholesterol
- 56 VP Virtual Patient
- 57 Vpop Virtual Population

58 3 Introduction

- 59 Physiologically based mathematical models are often used to describe and predict
- 60 the response of a patient to an existing therapy or novel agent. These models,
- 61 frequently referred to as quantitative systems pharmacology (QSP) models, are used
- 62 to simulate clinical trials in drug development (Musante, Ramanujan et al. 2017). In
- 63 these applications, it is important that they not only capture the mean patient
- 64 response to treatment but also inter-patient variability and how that variability may
- evolve over time. In addition, due to the novel nature of many therapies; the
- 66 complexity of human physiology; and generally limited human data, QSP models are
- 67 rarely fully determined by data. One approach to these challenges is to develop
- alternate parameter sets to capture the variability in the real clinical trial population
- and sample as much uncertainty in the model parameters as possible (Gadkar,
- 70 Budha et al. 2014, Hallow, Lo et al. 2014, van de Pas, Rullmann et al. 2014).
- 71
- 72 Previously, we published an algorithm for the generation and selection of these
- 73 alternative value sets (Allen, Rieger et al. 2016). The algorithm used simulated
- 74 annealing (SA) to generate as large a population of "plausible patients" (PPs) as was
- 75 practical. SA was used with a cost functional that optimized solutions to be
- 76 biologically feasible. These PPs, which we call a "plausible population", were termed
- 77 plausible since each generated parameter set simulated a patient that was
- 78 physiologically reasonable, and could be in a clinical trial, but there was not yet any
- selection for how *likely* it was for that patient to have been in a particular clinical
- 80 trial. We then used our novel selection technique to choose those patients from the
- 81 plausible population that most resembled a desired clinical population. These

- 82 selected patients were then termed virtual patients (VPs), and as a collection they
- 83 were called a virtual population (Vpop).
- 84 Since the original algorithm created a plausible population that was naïve to the
- 85 targeted Vpop distribution, significant computational effort was expended in
- 86 generating PPs in unlikely regions of the target distribution. Here we propose
- alternative algorithms to improve the generation of the plausible population for
- 88 more efficient generation of the Vpop. The common approach for each newly tested
- algorithms is to use information about the target distribution in generating the
- 90 plausible population. We explored this idea in three ways:
- 91 (1) Nested simulated annealing (NSA), which augments the SA method by
 92 targeting PP generation using the probability density function of the target
 93 distribution;
- 94 (2) A genetic algorithm (GA), which iteratively builds a plausible population
 95 according to a fitness function defined by the desired distribution; and lastly
- 96 (3) A Metropolis-Hastings (MH) inspired importance-sampling technique.

Results of the original SA method were re-generated, for direct comparison to eachof the three new approaches.

99 4 Methods

100 This current work is the evaluation of three approaches for the generation of Vpops 101 that match distributions of clinical cohorts or populations. The general flow for our

- 102 algorithm is (Figure 1):
- Implement an ordinary differential equation (ODE) model that describes the biological system of interest;
- For each state (variable) in the model, define a lower and upper limit for
 assessing if a steady state solution is plausible (all states between lower and
 upper limits) or not;
- 3. For each parameter of the model (e.g., rate constants, Michaelis-Menten constants), also define a plausible lower and upper limit for the search algorithms;
- 4. Optimize, using one of four algorithms, for solutions of the model that are
 PPs;
- 5. Collect the PPs generated by the optimization into a plausible population,
 terminating the search for PPs when the optimization achieves a preset
 number of PPs in the plausible population;
- 6. Perform acceptance/rejection sampling on the plausible population to select
 the VPs from the PPs that allow us to match the statistics of the target clinical
 population.

- 119 This section is organized to describe these three methods (NSA, modified GA, and
- 120 modified MH), and how to apply them to generate VPs. This is followed by a
- 121 description of how the results were analyzed, including a novel metric to quantify
- 122 the uniqueness of a collection of parameter sets.

123 4.1 Mathematical Model and Data

- 124 Following our previous approach, we tested our proposed methods using a
- 125 published ODE model of lipoprotein metabolism (van de Pas, Woutersen et al.
- 126 2012). In brief, the van de Pas model is a model of cholesterol production by the
- 127 liver and its transit through the plasma. The ODE cholesterol model has nine
- 128 equations, or state variables (Supplementary Table S1). These state variables
- 129 correspond to the mass or concentrations of species within particular
- 130 compartments (e.g., liver, plasma, peripheral tissues). The focus or primary outputs
- 131 of the model are calculating levels of high-density lipoprotein cholesterol (HDL_c)
- and "non-high-density lipoprotein cholesterol", which we assumed to be equivalent
- to low-density lipoprotein cholesterol (LDL_c). Thus the parameters of the ODE
- 134 model we changed in the global optimization methods were the rate constants of the
- 135 mass action model (e.g., production, reaction, clearance constants, see
- 136 Supplementary Table S2). For the present work of creating baseline PPs and VPs, we
- 137 only used the ODE model to simulate physiologically reasonable patients at steady
- 138 state and were not concerned with the transient changes of the model.
- 139 While the ODE model has nine states, not all of them are frequently collected in
- 140 clinical trials. The outputs of the model we matched to the statistics of human
- 141 clinical data through our Vpop selection algorithm were: HDL_c, LDLc, and total
- 142 cholesterol (TC). As in original paper, for our reference population to match we used
- 143 the National Health and Nutrition Examination Survey dataset (NHANES 2011-
- 144 2012). The NHANES dataset contained fasting values for plasma cholesterol levels
- in 2,942 patients. The data was well represented by a joint lognormal distribution
- 146 (Supplementary Figure S1).

147 4.2 Summary of Original SA Algorithm (Baseline Comparator)

148 In (Allen, Rieger et al. 2016) we optimized the steady-state solutions, x^* , to fall 149 within biologically reasonable ranges rather than to a specific point using the cost 150 functional

151
$$g(\mathbf{p}) = \sum_{i=1}^{N} \max\left[\left(x_i^*(\mathbf{p}) - \frac{l_i + u_i}{2} \right)^2 - \left(\frac{u_i}{2} - \frac{l_i}{2} \right)^2, 0 \right],$$
(1)

- 152 where *N* is the number of states of the model (N = 9 for van de Pas et al.), and l_i and
- 153 u_i represent the biologically plausible lower and upper bounds for the i^{th} state
- 154 variable's steady-state solution (see Supplementary Table S1). Note that if $x_i^*(\boldsymbol{p})$ is
- 155 within the plausible biological bounds, then $g(\mathbf{p}) = 0$, and the parameter set \mathbf{p} is
- 156 called a PP. SA iteratively proposes values of p until g(p) = 0. A new initial p is then
- 157 generated, and the SA optimization is repeated until a plausible population is

158 created.

159 4.3 NSA Algorithm

The NSA algorithm incorporates information about the target data distribution in
 the process of generating the plausible population. By modifying the cost functional,

- 162 equation (1), we can include information about the desired distribution, thus
- 163 decreasing the number of PPs required per VP. The joint distribution of NHANES
- patient's LDL_c, HDL_c, and TC is well approximated by a multivariate lognormal
 distribution, with a probability density function that is roughly ellipsoidal in iso
- distribution, with a probability density function that is roughly ellipsoidal in isodensity lines. The hypercube in which $q(\mathbf{p}) = 0$ in equation 1, was changed to an
- ellipsoidal shape, in the dimensions $x_i^*(\mathbf{p})$ that correspond to LDL_c, HDL_c, and TC.
- 168 The edge of this ellipsoid corresponds to the least-probable value (with respect to
- 169 the multivariate log-normal) for which $g(\mathbf{p}) = 0$.
- 170 However, the modified g(p) makes no distinction between low-probability solutions,
- 171 at the edge of the ellipse, and high-probability solution, near the centroid of the
- 172 ellipsoid. Hence, to fully use information from the target distribution, we considered
- 173 multiple nested ellipsoids, relegating acceptable PPs according to whether they
- achieve sufficiently high probability density with respect to this target distribution.
- 175 From this, the modified g(p) controls the number of PPs generated in each ellipse.
- 176 Note that while biological upper and lower bounds exist for all of the nine model
- 177 outputs, we only have distributional information regarding LDL_c, HDL_c, and TC. As a
- 178 result, the modified cost function still achieves a minimum when the remaining six

179 dimensions falls within the hypercube of biologically plausible solutions.

We use the following equation for the surface of an ellipsoid that will encompass thedata:

182
$$(X - \mu)^T \Sigma^{-1} (X - \mu) = c^2,$$
 (2)

183 where **X** is a 3×1 vector representing a point in the log-scaled vector of [LDL_c,

HDL_c, and TC], and μ and Σ are maximum likelihood estimates of the mean and

185 covariance matrix of the multivariate normal distribution, and c^2 controls the

186 extreme point of the ellipsoid. By letting **X** be the data point furthest from the mean

187 in (2), we can explicitly calculate the minimum value for c^2 that allows the data to

- 188 be encompassed by the ellipsoid.
- 189 First consider only one ellipsoid region. Then the modified cost functional is

190
$$h(\mathbf{p}) = g(\mathbf{p}) - \gamma((\mathbf{X} - \boldsymbol{\mu})^T \Sigma^{-1} (\mathbf{X} - \boldsymbol{\mu}) - c^2), \quad (3)$$

191 where $g(\mathbf{p})$ is given by equation (1) for N = 6, and is calculated for the 6 state

192 variables for which we do not have distributional information. We can interpret this

193 cost functional as forcing these 6 state variables to be within plausible biological

bounds while forcing the remaining 3 log-scaled observables to be within the

- 195 smallest ellipsoid region that encompasses the clinical data. Notice we have an
- 196 additional parameter, γ , which is a scaling factor that is a free parameter of the
- 197 method for balancing the weight of the ellipsoid term on the cost functional. A value
- 198 of $\gamma = 0.1$ was used for all simulations (Rieger and Allen 2017).
- 199 Now consider several nested ellipsoid regions. The cost functional for each nested ellipsoid is given in (3) but with modified c^2 values in order to control the 200
- distribution of the plausible population. The number of nested ellipsoids, *R*, is 201
- 202 another free parameter of this method. We denote the ellipsoids as $E_1 \subset E_2 \subset \cdots \subset$
- E_R , with the k^{th} ellipsoid centered at the mean $\boldsymbol{\mu}$ and defined as $E_k = \{\boldsymbol{X}: (\boldsymbol{X} \boldsymbol{\mu})^T \boldsymbol{\Sigma}^{-1} (\boldsymbol{X} \boldsymbol{\mu}) \leq c_k^2\}.$ 203
- 204
- We choose the c_k values such that a k/R proportion of the observations are within 205 the k^{th} ellipsoid: 206

207
$$\int_{E_k} \Phi(x) dx = \frac{k}{R} \quad , \tag{4}$$

where $\Phi(x)$ is the multivariate normal distribution, and $k = 1 \dots R$. We find an 208

209 approximate solution, c_k , to this integral, by using a Monte Carlo approach.

210 Equivalently,

211
$$\int_{E_1} \Phi(x) dx = \frac{1}{R}$$
 (5)

212
$$\int_{E_k \setminus E_{k-1}} \Phi(x) dx = \frac{1}{R}.$$
 (6)

213

For this method, we sequentially populate each ellipsoid uniformly such that the 214 215 final plausible population approximates the distribution for the target patient 216 distribution. We therefore need to calculate how many PPs are required for each ellipsoid, given a desired total number of PPs. Define q_k as the proportion of the 217 total plausible population within the k^{th} ellipsoid. Then, since we assume the data 218 219 are approximately uniformly distributed throughout each ellipsoid, we want to 220 solve a system of R equations for each q_k obtained by solving

221
$$\frac{1}{R} = \sum_{k=j}^{R} \frac{V_j - V_{j-1}}{V_k} q_k, \qquad (7)$$

for j = 1, ..., R. Where V_j is the volume of the j^{th} ellipsoid. We define $V_0 = 0$. Note 222 that $V_j \propto c_j^n$, where *n* is the dimension of the multi-dimensional distribution. Then, 223 equation (7) can be re-written as 224

(8)

 $\frac{1}{R} = \sum_{k=j}^{R} \frac{c_{j}^{n} - c_{j-1}^{n}}{c_{k}^{n}} q_{k},$ 225

which can be solved recursively for the q_k (starting with k = R, and defining $c_0^n = 227$ 0).

Alternatively, since the NHANES data provided individual level data, the target distributions c_k (and q_k) were calculated empirically, see source code (Rieger and

Allen 2017).

With the ellipsoids defined we can generate the plausible population by randomly

232 generating a parameter set in the ranges we defined from a uniform distribution.

Then, for a pre-defined plausible population of size m, for l = 1 to m, we identify a

234 PP by minimizing:

235
$$h_k(\mathbf{p}) = g(\mathbf{p}) - \gamma((\mathbf{X} - \boldsymbol{\mu})^T \Sigma^{-1} (\mathbf{X} - \boldsymbol{\mu}) - c_k^2), \quad (9)$$

where $g(\mathbf{p})$ is given by equation (1) for N = 6, and is calculated for the 6 state

variables for which we do not have distributional information. See SupplementaryText 1 for further details.

This method requires choosing the number of nested ellipsoids. The greater the number of ellipsoids, the closer the distribution of the plausible population will match that of the clinical population, thus reducing the number of PPs required per VP. However, an increases in the number of ellipsoids increases computation time for

- 242 VP. However, an increase in the number of ellipsoids increases computation time for
- the plausible population. In this case, we used five ellipsoids. We then use our
- rejection sampling method to select the VPs from the plausible population.

245 4.4 Modified GA

A commonly used population-based approach for optimizing nonlinear models is a
 genetic algorithm (GA), (Golberg 1989, Conn, Gould et al. 1991). For our problem,

248 we created our plausible population using MATLAB's *ga* function (MATLAB 2016).

This algorithm first creates an initial population, where each patient is drawn from a

250 uniform distribution. The algorithm then assigns a fitness value to each patient

using a cost (fitness) functional. Similar to the NSA method, we modify equation (1)

by incorporating information about the desired distribution. Specifically, the cost

253 functional is given by

254
$$H(\boldsymbol{p}) = \begin{cases} g(\boldsymbol{p}) & \text{if } g(\boldsymbol{p}) > 0\\ -\gamma(\boldsymbol{p}) & \text{otherwise,} \end{cases}$$
(10)

255 where $\gamma(\mathbf{p})$ is the likelihood of a given log-scaled observable value \mathbf{X} given by

256
$$\gamma(\boldsymbol{p}) = \frac{1}{\sqrt{(2\pi)^3 |\boldsymbol{\Sigma}|}} \exp\left(-\frac{1}{2} (\boldsymbol{X} - \boldsymbol{\mu})^T \boldsymbol{\Sigma}^{-1} (\boldsymbol{X} - \boldsymbol{\mu})\right). \quad (11)$$

This cost functional can be interpreted as forcing all state variables to be withinplausible biological bounds and additionally assessing a penalty as the log-scaled

259 observables deviate from μ .

As the algorithm progresses, children are created for each generation; those with a cost functional value $H(\mathbf{p}) < 0$ become PPs. Since many PPs are created each generation, there is no way to specify the exact number of PPs generated. Thus we must preset the minimum number of PPs desired, but in practice we tended to generate slightly more than sought (see Supplementary Code). Once the plausible population is created, we use rejection sampling to determine the Vpop from the plausible population.

267 4.5 Modified MH Algorithm

- The Metropolis-Hastings (MH) algorithm can be used to approximate a desired
- distribution, for a review see (Robert 2015). To apply the MH approach here we need to modify the algorithm. To see why, consider the original algorithm. Let $\pi(\mathbf{p})$
- be our desired target multivariate probability distribution for the vector \mathbf{p} . The MH
- algorithm generates a sequence of p, such that the distribution of this sequence,
- 273 $\{p_0, ..., p_N\}$ converges to $\pi(p)$ as samplings $\rightarrow \infty$. Let Q(p, q) be some symmetric
- 274 proposal distribution, which is interpreted as generating a proposed value **q** from
- 275 $Q(\mathbf{p}, \mathbf{q})$ when the process is at value **p**. Then the original MH algorithm is as follows:
- 276 1. Generate an initial vector p_0 , set i = 1.
- 277 2. Generate a proposed vector $\boldsymbol{p}^* \sim Q(\boldsymbol{p}_{i-1}, \boldsymbol{p}^*)$.
- 278 3. Calculate the probability \boldsymbol{p}^* is accepted, $\alpha = \min\left(1, \frac{\pi(\boldsymbol{p}^*)}{\pi(\boldsymbol{p}_{i-1})}\right)$.
- 4. Generate $Y \sim U(0,1)$, if $y \le \alpha$, set $p_i = p^*$. If $Y > \alpha$, set $p_i = p_{i-1}$.
- 280 5. Repeat steps 2 to 4 for i = 1, ..., number of samples to collect $\{p_0, ..., p_N\}$ as 281 a sampling from the target distribution.
- This MH algorithm approximates the target distribution $\pi(\mathbf{p})$ by randomly sampling from it. At first glance, this approach appears immediately applicable to the problem at hand and will generate a plausible population that will converge to the Vpop as $N \to \infty$. However, this algorithm requires modification because we do not know $\pi(\mathbf{p})$ a priori; i.e., we do not know how the parameters sets should be distributed
- such that the model, when simulated using those parameters, matches the data.
- We rewrite our target distribution as $T(X_p)$, where X is the observable outcomes generated by the model M, using a parameter set (which in this case is in the logspace, so $X_p = \log M(p)$). Then our algorithm becomes
- 291 1. Generate an initial vector p_0 , set i = 1.
- 292 2. Generate a proposed vector p_0 , set t = 1. 292 2. Generate a proposed vector $p^* \sim Q(p_{i-1}, p^*)$, write
- 293 $Q_m(p_{i-1}, p^*) = M(Q(p_{i-1}, p^*)).$

294 3. Calculate the probability
$$\boldsymbol{p}^*$$
 is accepted, $\alpha = \min\left(1, \frac{T(\boldsymbol{X}_{\boldsymbol{p}^*})Q_m(\boldsymbol{p}^*, \boldsymbol{p}_{i-1})}{T(\boldsymbol{X}_{\boldsymbol{p}_{i-1}})Q_m(\boldsymbol{p}_{i-1}, \boldsymbol{p}^*)}\right)$,

295 assume
$$\alpha \cong \min\left(1, \frac{T(X_{p^*})}{T(X_{p_{i-1}})}\right)$$

- 296 4. Generate $y \sim U(0,1)$, if $y \leq \alpha$, set $p_i = p^*$. If $y > \alpha$, set $p_i = p_{i-1}$.
- 297 5. Repeat steps 2 to 4 for i = 1, ..., N to collect $\{p_1, ..., p_N\}$ as a sampling from 298 the target distribution.

299 In the canonical version of the MH algorithm α is independent of the proposal 300 distribution *Q* because it is symmetric and cancels out of the equation. In the modified version above, Q_m is unknown and, in fact, is unlikely to be symmetric. In 301 order to proceed we assume that Q_m is approximately symmetric 302 $Q_m(\mathbf{p}^*, \mathbf{p}_{i-1}) \sim Q_m(\mathbf{p}_{i-1}, \mathbf{p}^*)$, so that we can calculate α as above. Because of this 303 304 approximation it is still necessary, following our previously published algorithm, to 305 apply acceptance-rejection sampling to finalize the Vpop from the plausible 306 population.

307 4.6 Assessing Similarity Between VPs

308 It is desirable to examine the parameter space in the Vpop to ensure heterogeneity

309 of the VPs (while still reproducing available data). The baseline method ensured this

310 diversity by generating VPs independently and from different initial parameter

311 estimates. However, this is not necessarily the case for the GA and MH methods.

To assess the diversity of a Vpop we devised a test metric $d(p_i, p_j)$ which scores

313 how similar two VPs are. By randomly sampling pairs of VPs from a given Vpop, we

built up a distribution for *d* and could compare the resultant cumulative density

function (CDF) for each method. The test metric *d* is simply the normalized dot-

316 product of p_i and p_j after they are scaled and shifted:

317
$$d(\boldsymbol{p}_{i}, \boldsymbol{p}_{j}) = \frac{\hat{\boldsymbol{p}}_{i}, \hat{\boldsymbol{p}}_{j}}{|\hat{\boldsymbol{p}}_{i}||\hat{\boldsymbol{p}}_{j}|}$$
$$\hat{\boldsymbol{p}} = \operatorname{diag}(\boldsymbol{V}^{-1}(\boldsymbol{p} - \boldsymbol{l})) - \frac{1}{2}$$
(12)

318 where **V** is a diagonal matrix such that $v_{ii} = u_i - l_i$. Hence, diag($V^{-1}(p - l)$) uses 210 the defined upper and lower bound for each normator (the elements of u and l

the defined upper and lower bound for each parameter (the elements of u and l

320 respectively), to scale each parameter in p to be between 0 and 1. To ensure that

- 321 $d \in [-1,1]$ we further subtract $\frac{1}{2}$ from each element. This means that, in principle, 322 \hat{p} can be orientated in any direction in *m*-dimensional space (where *m* is the
- p can be orientated in any direction in *m*-dimensional space (where *m* is the number of parameters). This also means that if the elements of **p** are sampled
- 324 uniformly between the upper and lower bounds that, by symmetry, the expected
- 325 value of the distribution should be zero (i.e., the CDF crosses 0.5 at d = 0). This is
- 326 the optimal parameter set in terms of diversity, but may not be achievable given the

327 constraints applied to the model. Conversely, if we generate Vpops from very similar

328 parameter sets then the distribution will be right-shifted towards d=1.

329 4.7 Assessing Goodness of Fit

- 330 The goodness of fit (GoF) to the empirical target distribution was assessed by using
- the Kolmogorov-Smirnov statistic for the marginal distribution over each
- 332 dimension:

333
$$GoF = \sum \sup |F_i(x) - D_i(x)|$$
(13)

- 334 where $F_i(x)$ is the empirical cumulative distribution function for the i^{th} model
- 335 observable that we are fitting the observed cumulative distribution of the data,

336 $D_i(x)$. Note that for a perfect fit GoF=0, and that GoF $\in [0, n]$, where *n* is the number 337 of distributions being fitted.

338 4.8 Source Code and Simulations

- All algorithms were implemented in MATLAB 2016b (v9.1) using the Global
- 340 Optimization Toolbox (v3.4.1) where a pre-packaged routine was available (e.g., GA,
- SA). The ODE model was implemented in SimBiology (v5.5). The K-S Test for GoF
- 342 utilizes MATLAB's Statistics and Machine Learning Toolbox (v11.0). The full source
- code is available for download from a GitHub repository (Rieger and Allen 2017).
- 344 The source code utilizes three independent packages from MathWorks File
- 345 Exchange (Johnson 2004, Jos 2016, Dorn 2017).
- 346
- 347 All simulations were performed sequentially on a MacBook Pro with a 2.9 GHz Intel
- Core i7 processor and 16 GB of RAM. For each choice of algorithm and pre-set
- number of PPs, simulations were repeated five times and the mean and standard
- 350 deviation calculated.

351 **5 Results**

352 **5.1 Comparing the various algorithms**

- 353 To compare the three proposed algorithms (NSA, GA and MH) we evaluated four
- 354 metrics to measure performance of the algorithm compared to the original SA
- 355 method. For each algorithm, we evaluated:
- Efficiency: How many PPs were needed to achieve a certain GoF of the final
 Vpop to the observables?
- 2. **Computational Cost:** How fast was the generation of PPs and VPs?
- 3593. Diversity: Are the VPs parametrically similar or do they maintain theparametric heterogeneity of the PPs?
- 3614. Convergence: Do the methods benefit from the acceptance/rejection step or can a Vpop be generated directly?

363 **5.2** Comparison of algorithms for efficiency of yield

364 For each algorithm, we targeted generation of between 100 and 7,500 total PPs;

those PPs were then converted into VPs through the acceptance/rejection

algorithm. The GoF of the resulting Vpop was calculated as discussed in Methods. By

367 comparing the GoF achieved for the Vpops with varying PPs (Figure 2) we find that

as the number of PPs \rightarrow 5,000+, all of the algorithms generated essentially

369 indistinguishable GoFs for the final Vpop (albeit with different VPs in each Vpop).

370 However, the three new algorithms were more efficient than the original SA method,

371 especially when the number of PPs < 1,000. In fact, Vpops generated with as few as

100 PPs could have similar fits to the observable data as the SA method with 500+

373 PPs.

5.3 Comparison of algorithms for computational cost

Even if an algorithm can generate the same GoF through far fewer PPs than the

376 original SA algorithm, this does not necessarily mean the process was

377 computationally more efficient. We further compared each method based on the

378 clock time (evaluated via MATLAB's *tic/toc* functions) required to generate a Vpop

from 7,500 PPs (Figure 3). While the NSA method was arguably superior based on

380 yield, this algorithm required approximately the same amount of time to execute as

the SA method. Based on time, the MH and GA were the fastest algorithms and the

382 SA remains among the least efficient.

5.4 Comparison of algorithms for parametric diversity of the final Vpop

384 An advantage of the SA algorithm is its ability to generate Vpops that maintain most 385 of the parametric diversity of the original PPs (Supplementary Figure S2-3). This diversity in the Vpop is an essential feature for QSP models since they are often 386 387 utilized in simulation of clinical trials involving novel therapies. If the underlying 388 parameters of VPs are highly similar/correlated, clinical trial simulations performed 389 with the Vpop may incorrectly predict a very narrow range of therapeutic response. 390 Therefore, we need to ensure that as we introduce new algorithms, we do not trade 391 parametric diversity for computational gains. We measured the diversity of the 392 Vpops generated by each algorithm by uniformly sampling pairs of VPs and 393 calculating the dot product between each set of parameters (see Methods). As a 394 reference point/positive control, we included a set of uniformly, randomly 395 generated model parameters (Figure 4). The closer each algorithm's final VP 396 parameter distribution is to the random reference, the more diverse we considered 397 the set of VPs in the Vpop. For this criterion, the SA method was found to have the 398 most diversity, indistinguishably followed by NSA and MH. The GA method showed 399 distinct rightward shifts in its distribution, indicating that fewer independent 400 parameter sets were identified in the generation of the Vpops. Supplementary 401 figures show the violin plot for each method for both the PPs and VPs for a single 402 iteration (Supplementary Figures S3, S5, S7, and S9).

403 5.5 Convergence of the algorithms to the data

404 In contrast to the original SA method, each of the methods tested use information about the desired population distribution and thus requires fewer PPs to achieve an 405 406 acceptable fit for the Vpop (Figure 2). To evaluate if the final selection step was still 407 required as part of the algorithm workflow, we compared the GoF for each of the 408 methods before and after the acceptance/rejection step, starting with \sim 7,500 PPs in 409 each case (Figure 5). As expected, the largest improvement in Vpop fit from the PPs 410 to VPs was for the SA method; however, all of the methods showed at least a 3-fold improvement in GoF through the final selection step. The NSA method showed the 411 412 best initial fit for its PPs to the NHANES data, reasonably reproducing both the 1-413 dimensional and 2-dimensional histograms before the selection step (Figure S3A-F).

- These fits were approximately equivalent to the final Vpop fit for the SA method
- 415 starting with 1,000 PPs.

416 6 Discussion

- 417 By design, most quantitative systems pharmacology models are not identifiable
- 418 from available data. While it would be desirable to have parameters well
- 419 determined and characterized, the uncertainty in parameter values in QSP models
- 420 often reflects our current knowledge (or lack thereof) of human (patho)-physiology.
- 421 Therefore, with this perspective, we can use these models in a hypothesis-
- 422 generation/testing mode to explore how these knowledge gaps translate to
- 423 uncertainties in clinical outcomes and clinical trial design. In our opinion, the most
- thorough and robust way of doing this is by generating the most diverse Vpops
- 425 given the available data.
- 426 Exploring the parameter space of under-determined quantitative systems
- 427 pharmacology models remains a challenge but it is essential for robust predictions
- 428 of safety and efficacy for novel compounds. Here we presented three methods for
- 429 generating diverse parameter sets in a QSP model. While this exercise is by no
- 430 means an exhaustive exploration of global optimization techniques, each algorithm
- 431 improved at least one of the testing metrics compared to our previously published
- 432 SA method. The seemingly simple question of which method is "the best" cannot be
- 433 definitively answered here but it is important to be aware of the pros and cons for
- 434 each and potential steps to improve performance.
- 435 We previously discussed the advantages and disadvantages of using the SA method
- 436 for this application (Allen, Rieger et al. 2016). In comparison to other methods
- 437 tested it was the slowest (or tied with NSA) and required the most PPs for a quality
- 438 fit. Conversely, it also generated the most diverse Vpop with the fewest imposed
- 439 correlations. The ease of implementation is also an advantage for SA. As
- implemented, the algorithm required no prior knowledge of the final Vpop
- distribution and there was a minimal set of tuning parameters required, most of
- 442 which were default MATLAB options (i.e., no arbitrary decision about number of

ellipsoids, number of generations). As such, the algorithm remains relevant as a

444 "first try" for generating VPs. Furthermore, it is the only method that can be run (at

least in part) without prior knowledge of the target distribution. This relaxed

446 requirement can make it an attractive choice for pre-computing plausible

447 populations or for exploring how the parameter space relates to the model output

448 (for example, identifying parameters in the model that can give rise to sub-

449 populations of interest).

450 The NSA approach iterates on the SA method by utilizing prior knowledge of the

451 final parameter distribution and forcing the algorithm to regions with the most

452 desired patient density. This method is likely most efficient when the target

453 distribution is approximately multivariate normal. Fortunately, for the example

here, the target distribution was well approximated as a multivariate lognormal.
The viability of this method for more eccentric or bimodal distributions would need

456 to be studied by applying it to other case studies. However, such distributions are

457 less commonly observed in clinical trials. For our case study, the computational cost

458 to generate a plausible population was comparable between the NSA and SA

459 methods; however, the NSA approach demonstrated vastly improved yield (VP per

460 PP), which facilitated an overall more efficient Vpop generation process. The

algorithm was as good, or better, than the other methods tested for direct

462 generation (pre-selection/rejection) of a reasonable Vpop, without the imposed

463 correlations found in Vpops generated by GA. While essentially the same as the SA

464 method to implement, there is a problem-specific choice for the number of ellipsoids

to use. Here we used five regions, regardless of the number of PPs being generated.

Fine-tuning based on the model/number of PPs may potentially improve

467 performance.

468 MH is unique amongst the approaches we tried in that it is a Markov Chain, which 469 should imply some degree of correlation between the PPs. The advantage of this 470 technique was an increase in speed and compared to the two methods based on SA; 471 however, there also was a right-shift in the dot product cumulative distribution. 472 implying a slightly less diverse final population. Methods have been published to 473 attempt to reduce this correlation (Santoso, Phoon et al. 2011) and to improve 474 performance in higher dimensions (Betancourt 2017), but we chose to evaluate only 475 the common form of the algorithm and to leave further exploration for future 476 improvements. While straightforward to implement, MH requires the choice of a 477 proposal distribution. As noted in the Methods, because we indirectly sample the 478 distribution of the observables by first sampling the parameter space and then 479 generate the observables through model simulation we do not have direct control 480 over the choice of a proposal distribution. The implications of this for direct 481 convergence of this method will depend on the symmetry of the observable 482 distribution (induced by the parameter sampling) around every point on the 483 Markov chain. In this case, the approximation we assumed (see Methods) appeared 484 to hold sufficiently for the MH algorithm to approximate the empirical distributions. 485 However, the final Vpop was improved by acceptance/rejection sampling.

486 The GA was very similar to MH in that, compared to the SA-based methods, a 10-fold

487 improvement in computational speed was achieved at the cost of some lost

- 488 heterogeneity in the final Vpop. The GA is easy to implement for OSP models and the
- 489 supplied routine with MATLAB's Global Optimization Toolbox was sufficient for our
- 490 purposes. GA requires some problem-specific decisions, which may affect overall
- 491 performance; for example, the size of the population, number of generations, and
- 492 mutation rate can be adjusted as needed.
- 493 The curse of under-determined models has led to a long history of using different
- 494 global optimization techniques for generating parameter sets within the bounds of
- 495 the data (van de Pas, Woutersen et al. 2012, Gadkar, Budha et al. 2014, Hallow, Lo et
- 496 al. 2014). Use of global optimization techniques often feels like more of an art than a
- 497 science due to how problem-specific their application can be. For this reason, we 498
- examined several algorithms with different approaches for exploring constrained, 499 multidimensional parameter spaces. Requiring only minimal tuning, each of these
- 500 algorithms successfully explored the range of our 23-dimensional parameter space
- 501 and generated reasonable PPs. The choice of algorithm to use for a new problem,
- 502 particularly one with higher dimensions and a less Gaussian set of observations, will
- 503 need to be evaluated on a case-by-case basis. For example, for models that are slow
- 504 to simulate the most constraining factor is computational cost. In this case the MH
- 505 or GA approaches may be the most successful; however, as we have shown, without
- 506 adaptation these methods may come at a cost of diversity in the final Vpop.
- 507 We hope that the results presented here will provide a guide to selection and implementation of these algorithms to facilitate the generation of robust Vpops in 508
- 509 mathematical models of (patho)-physiology.

7 Author contributions 510

- 511 RJA conceived of the original algorithm. CJM, RJA, and TRR conceived of the updated 512 algorithm objectives. AG, GWC, LB, RW, YC1, YC2, and YL selected and coded the new 513
- algorithms and performed the initial proof-of-concept testing. CJM, RE, HTB, RJA,
- 514 and TRR supervised and advised the initial work. RJA, RE, RW, TRR, HTB, and CJM
- 515 drafted the manuscript. All authors reviewed, revised, and approved of the final
- 516 manuscript.

8 Conflict of interest 517

- TRR, RJA, and CJM were employees of Pfizer Inc. during the completion and 518
- 519 analysis of this study.

9 Funding 520

- 521 This research was supported in part by the National Institute on Alcohol Abuse and
- Alcoholism under grant number 1R01AA022714-01A1, in part by the Air Force 522
- 523 Office of Scientific Research under grant number AFOSR FA9550-15-1-0298, and in

- 524 part by the US Department of Education Graduate Assistance in Areas of National
- 525 Need (GAANN) under grant number P200A120047. GWC was supported by the
- 526 Clarendon fund and EPSRC. Pfizer Inc. supported the research of TRR, RJA, and CJM.

527 **10 Acknowledgements**

- 528 The authors thank Ilse Ipsen and Thomas Gehrmann for organizing the 2016 SAMSI
- 529 Workshop at North Carolina State University, which initially facilitated this 530 collaboration.

531 **11 References**

- Allen, R. J., T. R. Rieger and C. J. Musante (2016). "Efficient Generation and Selection
- 533 of Virtual Populations in Quantitative Systems Pharmacology Models." <u>CPT</u>
- 534 Pharmacometrics Syst Pharmacol **5**(3): 140-146.
- 535 Betancourt, M. (2017) "A Conceptual Introduction to Hamiltonian Monte Carlo."
- 536 <u>ArXiv e-prints</u> **1701**, 60.
- 537 Conn, A. R., N. I. Gould and P. Toint (1991). "A globally convergent augmented
- Lagrangian algorithm for optimization with general constraints and simple bounds."
 SIAM Journal on Numerical Analysis 28(2): 545-572.
- 540 Dorn, J. (2017). Violin Plots for plotting multiple distributions (distributionPlot.m).
- 541 <u>https://www.mathworks.com/matlabcentral/fileexchange/23661-violin-plots-for-</u> 542 <u>plotting-multiple-distributions--distributionplot-m-</u>, MathWorks File Exchange.
- 543 Gadkar, K., N. Budha, A. Baruch, J. D. Davis, P. Fielder and S. Ramanujan (2014). "A

544 Mechanistic Systems Pharmacology Model for Prediction of LDL Cholesterol

- 545 Lowering by PCSK9 Antagonism in Human Dyslipidemic Populations." <u>CPT</u>
- 546 <u>Pharmacometrics Syst Pharmacol</u> **3**: e149.
- 547 Golberg, D. E. (1989). <u>Genetic algorithms in search, optimization, and machine</u>
 548 <u>learning.</u> Reading, MA, Addison-Wesley Publishing Co.
- Hallow, K. M., A. Lo, J. Beh, M. Rodrigo, S. Ermakov, S. Friedman, H. de Leon, A.
- 550 Sarkar, Y. Xiong, R. Sarangapani, H. Schmidt, R. Webb and A. G. Kondic (2014). "A
- model-based approach to investigating the pathophysiological mechanisms of
- by 552 hypertension and response to antihypertensive therapies: extending the Guyton
- 553 model." <u>AJP: Regulatory, Integrative and Comparative Physiology</u> **306**(9): R647-
- 554 R662.
- 555 Johnson, A. (2004). error_ellipse.
- 556 <u>http://www.mathworks.com/matlabcentral/fileexchange/4705-error-ellipse</u>,
- 557 MathWorks File Exchange.

bioRxiv preprint doi: https://doi.org/10.1101/196089; this version posted January 18, 2018. The copyright holder for this preprint (which was not certified by peer review) is the author/funder, who has granted bioRxiv a license to display the preprint in perpetuity. It is made available under aCC-BY-ND 4.0 International license.

- 558 Jos (2016). ALLCOMB All combinations.
- 559 https://www.mathworks.com/matlabcentral/fileexchange/10064-allcomb-
- 560 <u>varargin-</u>, MathWorks File Exchange.
- 561 MATLAB (2016). MATLAB and Global Optimization Toolbox Release 2016b. Natick,
- 562 Massachussetts, USA.
- 563 Musante, C. J., S. Ramanujan, B. J. Schmidt, O. G. Ghobrial, J. Lu and A. C.
- 564 Heatherington (2017). "Quantitative Systems Pharmacology: A Case for Disease
- 565 Models." <u>Clin Pharmacol Ther</u> **101**(1): 24-27.
- 566 NHANES. (2011-2012). "National Health and Nutrition Examination Survey
- 567 (NHANES) Data." 2011-2012. from http://www.cdc.gov/nchs/nhanes.htm.
- 568 Rieger, T. and R. Allen (2017). vpop-gen. <u>https://doi.org/10.5281/zenodo.1117870</u>,
 569 Pfizer Inc.
- Robert, C. P. (2015). "The Metropolis-Hastings algorithm." <u>ArXiv e-prints</u> 1504:
 arXiv:1504.01896.
- 572 Santoso, A., K. Phoon and S. Quek (2011). "Modified Metropolis–Hastings algorithm
- with reduced chain correlation for efficient subset simulation." <u>Probabilistic</u>
 Engineering Mechanics **26**(2): 331-341.
- 575 van de Pas, N. C. A., J. A. C. Rullmann, R. A. Woutersen, B. van Ommen, I. M. C. M.
- 576Rietjens and A. A. de Graaf (2014). "Predicting individual responses to pravastatin
- 577 using a physiologically based kinetic model for plasma cholesterol concentrations."
- 578 Journal of Pharmacokinetics and Pharmacodynamics **41**(4): 351-362.
- van de Pas, N. C. A., R. A. Woutersen, B. van Ommen, I. M. C. M. Rietjens and A. A. de
- 580 Graaf (2012). "A physiologically based in silico kinetic model predicting plasma
- 581 cholesterol concentrations in humans." <u>The Journal of Lipid Research</u> **53**(12): 2734-
- 582 2746.
- 583 12 Figure Captions
- 584

bioRxiv preprint doi: https://doi.org/10.1101/196089; this version posted January 18, 2018. The copyright holder for this preprint (which was not certified by peer review) is the author/funder, who has granted bioRxiv a license to display the preprint in perpetuity. It is made available under aCC-BY-ND 4.0 International license.

12.1 Flowchart of algorithm 585

586

587 Figure 1. Flowchart of algorithm. The initial problem setup is shared by each of the 588 methods attempted, where biologically plausible ranges are placed on model 589 parameters and states. Once the problem is setup, the generation of plausible

590 patients is carried out by one of four algorithms. Post-plausible-patient generation,

- 591 each algorithm follows the same acceptance/rejection sampling steps to create the
- 592 virtual population.
- 593 12.2 Goodness-of-fit vs. number of plausible patients
- 594

595 Figure 2. Goodness-of-fit (lower number is better) of the final virtual population vs.

596 the number of plausible patients generated for each method. Shown is

597 mean±standard deviation of 5 runs. SA = simulated annealing (blue circles), NSA =

598 nested simulated annealing (red squares). MH = Metropolis-Hastings (vellow

- 599 diamonds), GA = genetic algorithm (purple x's).
- 600 12.3 Comparison of VP and PP generation time for each method
- 601

602 Figure 3. Comparison of the time/plausible patient (open bars) or time/virtual

603 patient (filled bars) for each method. For each method, \sim 7,500 plausible patients

604 were generated and then a virtual population was selected from those plausible

605 patients. Shown is mean±standard deviation of 5 runs. Time was calculated via the

606 functions *tic/toc* in MATLAB. SA = simulated annealing (blue), NSA = nested

607 simulated annealing (red), MH = Metropolis-Hastings (yellow), GA = genetic 608 algorithm (purple).

- 609 **12.4** Diversity of VPs in final Vpops
- 610

611 Figure 4. Cumulative distribution vs. the dot-product of the vector of virtual

612 patients' (VPs) parameters to assess the diversity of parameter values in the virtual

613 population. For each method, 50,000 dot-products of randomly chosen VPs were

calculated and the cumulative distribution plotted. Shown is mean±standard 614

615 deviation of 5 runs. As a positive control, a set of parameters from a uniform

distribution was generated (solid, black line). Distributions closer to the uniform 616

- 617 random control indicate a more diverse set of VPs. Distributions skewed towards
- 618 the right indicates a more uniform set of VPs. SA = simulated annealing (blue circles,
- 619 solid), NSA = nested simulated annealing (red squares, dashed), MH = Metropolis-

620 Hastings (yellow diamonds, dotted), GA = genetic algorithm (purple x's, dashed).

- 621 12.5 Efficiency of the acceptance/rejection algorithm
- 622

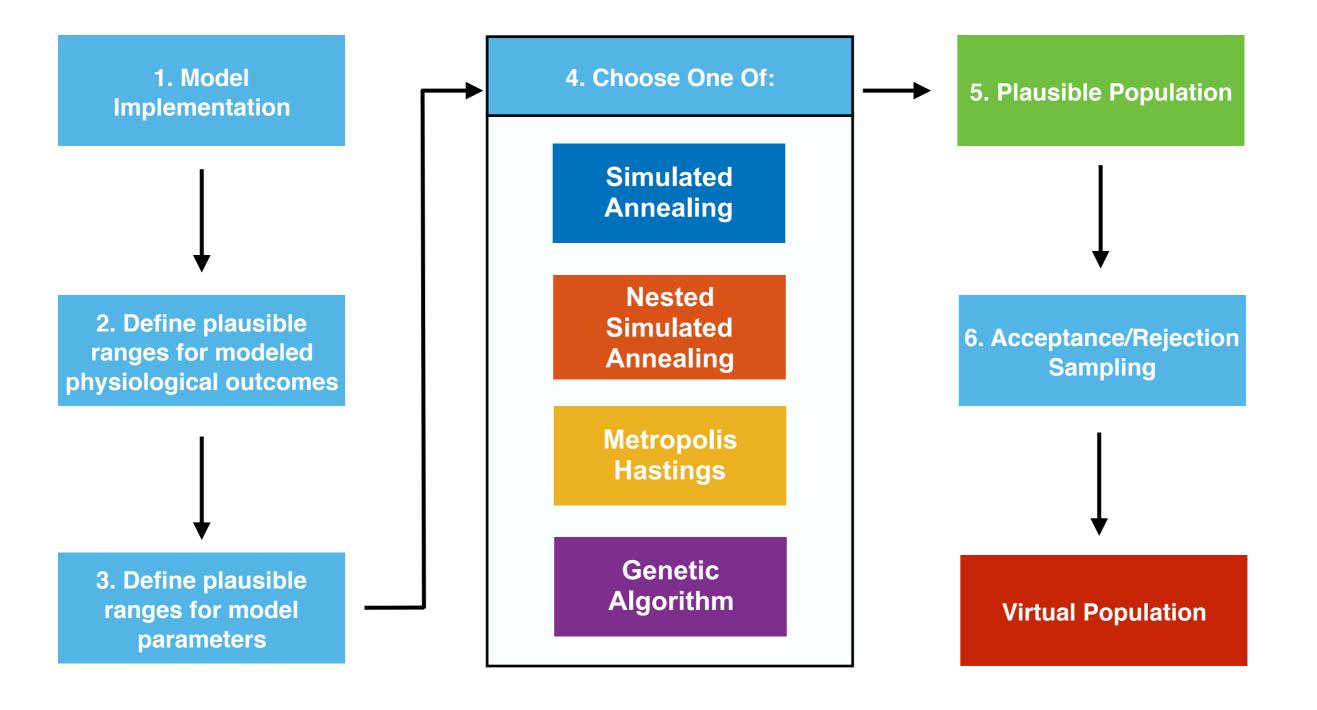
Figure 5. Improvement of goodness-of-fit (lower number is better) from the 623

- plausible patients (open bars) \rightarrow virtual patients (filled bars) for each method 624
- 625 starting from \sim 7,500 plausible patients. Shown is mean±standard deviation of 5

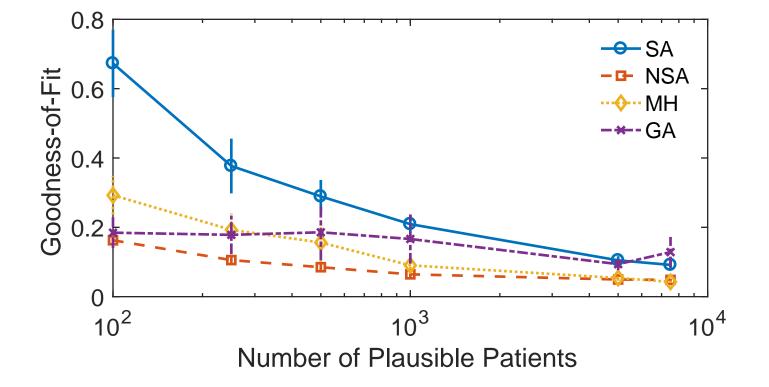
bioRxiv preprint doi: https://doi.org/10.1101/196089; this version posted January 18, 2018. The copyright holder for this preprint (which was not certified by peer review) is the author/funder, who has granted bioRxiv a license to display the preprint in perpetuity. It is made available under aCC-BY-ND 4.0 International license.

- runs. SA = simulated annealing (blue), NSA = nested simulated annealing (red), MH
- 627 = Metropolis-Hastings (yellow), GA = genetic algorithm (purple).

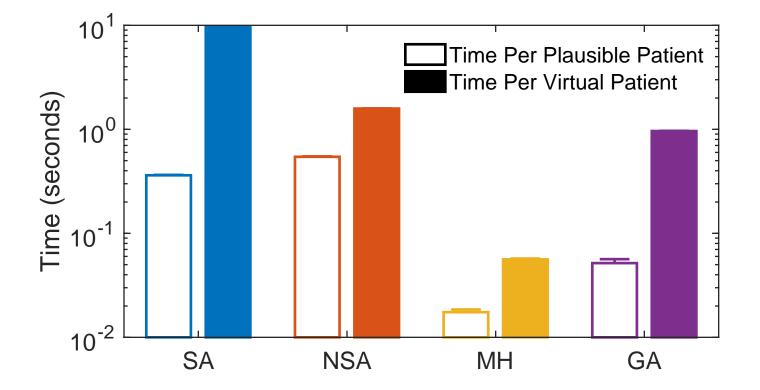
acc-BY-ND 4.0 International license.



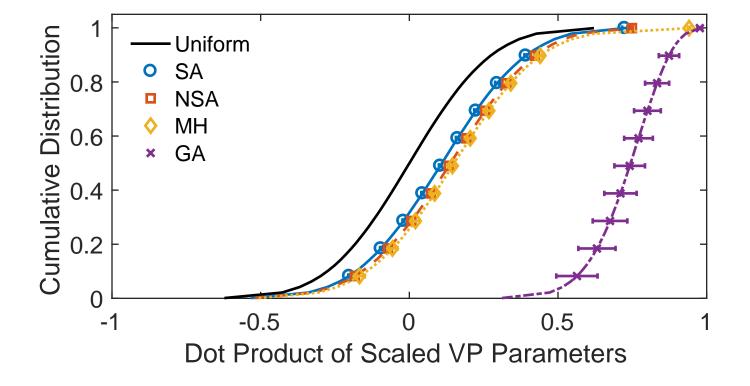
bioRxiv preprint doi: https://doi.org/10.1101/196089; this version posted January 18, 2018. The copyright holder for this preprint (which was not certified by peer review) is the author/funder, who has granted bioRxiv a license to display the preprint in perpetuity. It is made available under aCC-BY-ND 4.0 International license.



bioRxiv preprint doi: https://doi.org/10.1101/196089; this version posted January 18, 2018. The copyright holder for this preprint (which was not certified by peer review) is the author/funder, who has granted bioRxiv a license to display the preprint in perpetuity. It is made available under aCC-BY-ND 4.0 International license.



bioRxiv preprint doi: https://doi.org/10.1101/196089; this version posted January 18, 2018. The copyright holder for this preprint (which was not certified by peer review) is the author/funder, who has granted bioRxiv a license to display the preprint in perpetuity. It is made available under aCC-BY-ND 4.0 International license.



bioRxiv preprint doi: https://doi.org/10.1101/196089; this version posted January 18, 2018. The copyright holder for this preprint (which was not certified by peer review) is the author/funder, who has granted bioRxiv a license to display the preprint in perpetuity. It is made available under aCC-BY-ND 4.0 International license.

